Effects of Δ-isobar degrees of freedom on low-energy electroweak transitions in few-body nuclei

R. Schiavilla and R. B. Wiringa
Physics Division, Argonne National Laboratory, Argonne, Illinois 60439

V. R. Pandharipande
Department of Physics, University of Illinois, Urbana, Illinois 61801

J. Carlson
Theory Division, Los Alamos National Laboratory, Los Alamos, New Mexico 87545
(Received 25 November 1991)

Variational wave functions with Δ-isobar components are used to study trinucleon magnetic moments, the Gamow-Teller matrix element of tritium β decay, thermal neutron radiative capture on ^{3}He, and low-energy proton weak capture on ^{3}He. The Δ-isobar components are generated by transition correlation operators acting on realistic nuclear wave functions. These correlations are obtained from a fit to exact two-body ground-state and low-energy scattering solutions for the Argonne v_{28} and v_{28Q} interaction models, which include Δ-isobar degrees of freedom. Contributions of Δ isobars to electroweak current operators appear at the one-body level in this formalism. Their effect on low-energy electroweak transitions is significantly smaller than that obtained in perturbation theory analyses, where Δ-isobar effects are commonly subsumed into effective two-body current operators. The resulting theoretical cross section for thermal neutron radiative capture on ^{3}He is ≈ 86 μb, compared to an experimental value of 55 ± 3 μb; the astrophysical S factor for proton weak capture on ^{3}He is predicted to be in the range $(1.4-3.2)\times10^{-23}$ MeV b.

PACS number(s): 24.80.−x, 21.45.+v, 21.30.+y

I. INTRODUCTION

The radiative ^{3}He$(n,\gamma)^4$He and weak ^{3}He$(p,e^+\nu_e)^4$He capture reactions at thermal neutron and keV proton energies are interesting in that their cross sections are very sensitive to the model used to describe both the ground-state and continuum wave functions, and the two-body electroweak current operators [1–6]. This is because the single-nucleon electromagnetic or axial current operator cannot connect the main S-state components of the ^{3}He and ^{4}He wave functions at low energies. Hence in impulse approximation the calculated cross section is small, since the reaction must proceed through the small components of the wave functions. However, the exchange current operator can connect the S-state components, and its matrix element is exceptionally large in comparison with that obtained in impulse approximation.

Two groups, Wervelman *et al.* [4] and Wolfs *et al.* [7], have recently measured the ^{3}He$(n,\gamma)^4$He cross section; they quote values of 55 ± 3 and 54 ± 6 μb, respectively, in good agreement with each other and with two earlier measurements [8,9], although not with the smaller value reported in Ref. [10]. The ^{3}He$(p,e^+\nu_e)^4$He cross section cannot be measured in the energy range relevant for solar fusion. The possibility that the small neutrino flux associated with this reaction (the H*ep* neutrinos) might be detectable in the new generation of solar neutrino experiments makes an accurate theoretical prediction highly desirable [11].

Most of the previous calculations of the ^{3}He$(n,\gamma)^4$He and ^{3}He$(p,e^+\nu_e)^4$He reactions have been based on shell model descriptions of the initial- and final-state nuclear wave functions, and the Chemtob-Rho prescription [12] (with some short-range modification) for the two-body components in the electroweak current operator [1–4]. These calculations have led to contradictory results. For example, in the radiative capture reaction, Towner and Khanna [2] have found that the cross section is dominated by exchange current contributions, whereas Tegnér and Bargholtz [3], and more recently Wervelman *et al.* [4], have found that these contributions provide only a small correction to the cross-section value obtained in impulse approximation. Furthermore, large differences exist even between the impulse approximation (IA) values: Towner and Khanna quote results ranging from 2 to 14 μb depending on whether harmonic oscillator or exponential wave functions are used to describe the ^{3}He and ^{4}He ground states. However, Wervelman *et al.* quote an IA cross section of 50 μb. These discrepancies are presumably due to the schematic wave function models used in the calculations.

In an attempt to reduce the uncertainties in the predicted values for both the radiative and weak capture rates, we recently performed a fully microscopic calculation of these reactions, based on ground-state and continuum wave functions obtained from a realistic Hamiltonian with two- and three-nucleon interactions [5,6]. Both correlation and initial-state interaction effects were thus included. Furthermore, the main part of the two-body electromagnetic current operator (denoted as "model independent") was constructed consistently from the two-nucleon interaction model with the methods developed in

Refs. [5,13,14]. The less-well-known electroweak currents associated with the excitation of an intermediate Δ isobar, and the $\rho\pi\gamma$ and $\omega\pi\gamma$ electromagnetic couplings (denoted as "model dependent") were also included. However, it was emphasized that their contribution should be viewed as numerically uncertain, as very little empirical information is available on their coupling constants and short-range behavior. These studies showed that both reactions have large (in the case of radiative capture, dominant) contributions from two-body current operators. Indeed, the calculated IA and total values for the cross section of the radiative capture (astrophysical S factor of the weak capture) were 6 and 112 μb (5.8×10^{-23} and 1.3×10^{-23} MeV b), respectively. This was in sharp contrast with results reported in the two most recent shell model calculations [3,4]. Our results also indicated that the common practice of inferring the astrophysical S factor of the weak capture from the measured radiative capture cross section is bound to be misleading because of different initial-state interactions in the $n+{}^3$He and $p+{}^3$He channels, and because of the large contributions associated with the two-body components of the electroweak current operator.

The substantial overprediction of the $n+{}^3$He capture cross section obtained in Ref. [5] was unsatisfactory, however. The "model-dependent" contributions, particularly those due to the Δ-isobar current, seemed unreasonably large. For example, the Δ-isobar current contribution to the radiative capture was about 30 μb, or 27% of the total calculated value. In the present work the Δ-isobar degrees of freedom are explicitly included in the nuclear wave functions, rather than being eliminated in favor of effective two-body operators acting on nucleon coordinates, as is commonly done in perturbative treatments [2–6,15–17]. Thus the present calculation is along the lines of the coupled-channel approach of Refs. [18–20] in the two-body system, and of Ref. [21] in the three-body system. However, one- and two-Δ components are retained in the three- and four-body wave functions, in contrast to Ref. [21], where the nucleon and Δ-isobar Hilbert space was truncated at the one-Δ level.

The correlation operator method is used to generate the one- and two-Δ components. The $NN\rightarrow N\Delta$ or ΔN and $NN\rightarrow\Delta\Delta$ transition correlation operators are obtained from two-body ground-state and low-energy scattering solutions for the Argonne v_{28} and v_{28Q} interaction models [22], which have explicit Δ-isobar degrees of freedom, and fit the available NN scattering data at $E_{\rm lab}\leq400$ MeV. The correlation operator method has been shown to provide high-quality trial functions for use in variational calculations of light nuclei with nucleon degrees of freedom [23]. It is reviewed and generalized to the case of Δ-isobar degrees of freedom in Sec. II. The expressions for the $N\rightarrow\Delta$ transition and Δ-electroweak current operators are given in Sec. III, while the calculation of the required matrix elements is discussed in Sec. IV. The results for the trinucleon magnetic moments, the Gamow-Teller matrix element of tritium β decay, the thermal neutron radiative capture on ^{3}He, and the low-energy proton weak capture on ^{3}He are presented in Sec. V. Finally, a concluding discussion is given in Sec. VI.

II. THE CORRELATION OPERATOR METHOD

The correlation operator (CO) method has proven very useful in the variational theory of light nuclei [13,23–27]. We will first briefly review the method used with only the nucleon degrees of freedom, and then discuss its generalization to include the Δ-isobar degrees of freedom. In the simplest version of the CO method the variational wave function for light nuclei is taken as [24–26]

$$|\Psi_v\rangle=\left[S\prod_{i<j}(1+U_{ij})\right]\left[\prod_{i<j}f^c(r_{ij})\right]|\Phi\rangle\ . \tag{2.1}$$

Here Φ is an uncorrelated spin-isospin wave function, and the $f^c(r_{ij})$ are two-body spatial correlations which keep the particles apart at short distances, to avoid the repulsive core of the NN interaction, while at large distances they fall off to provide confinement. The U_{ij} are two-body spin and tensor correlations,

$$U_{ij}=u^\sigma(r_{ij})\boldsymbol{\sigma}_i\cdot\boldsymbol{\sigma}_j+u^{t\tau}(r_{ij})S_{ij}(\boldsymbol{\tau}_i\cdot\boldsymbol{\tau}_j)\ , \tag{2.2}$$

and S is a symmetrizer because the operators do not commute. The $f^c(r_{ij})$ and $u^{t\tau}(r_{ij})$ are shown in Fig. 1 for ^{2}H, ^{3}He, and ^{4}He. The U_{ij} generally have very little A dependence.

The $f^c(r_{ij})$, $u^\sigma(r_{ij})$, and $u^{t\tau}(r_{ij})$ are determined by minimizing the energy. In practice it is very convenient to relate them to two-body wave functions in ${}^1S_0$ and ${}^3S_1$-${}^3D_1$ channels:

$$f({}^1S_0,r)=[1-3u^\sigma(r)]f^c(r)\ , \tag{2.3}$$

$$f({}^3S_1,r)=[1+u^\sigma(r)]f^c(r)\ , \tag{2.4}$$

$$f({}^3D_1,r)=-3\sqrt{8}u^{t\tau}(r)f^c(r)\ , \tag{2.5}$$

which are solutions of the two-body Schrödinger equations:

$$\left[-\frac{\hbar^2}{m}\nabla^2+v({}^1S_0,r)+\lambda({}^1S_0,r)\right]f({}^1S_0,r)\mathcal{Y}^0_{000}=0\ , \tag{2.6}$$

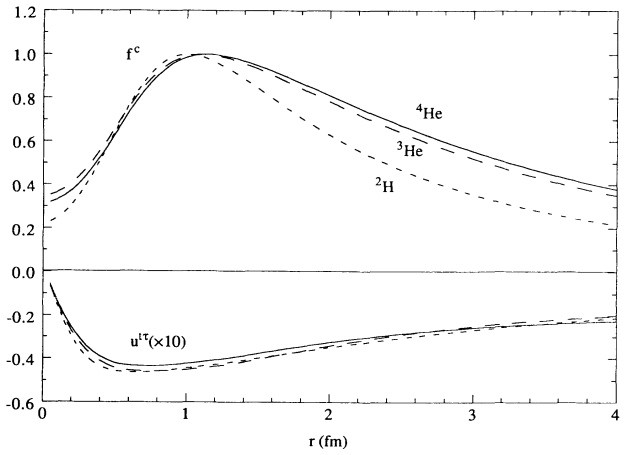

FIG. 1. The $f^c(r)$ and $u^{t\tau}(r)$ correlations for ^{2}H, ^{3}He, and ^{4}He with the Argonne v_{14} + Urbana VIII Hamiltonian.

$$\left[-\frac{\hbar^2}{m}\nabla^2+v(^3S_1\text{-}^3D_1,r)+\lambda(^3S_1\text{-}^3D_1,r)\right]$$
$$\times[f(^3S_1,r)\mathcal{Y}^m_{011}+f(^3D_1,r)\mathcal{Y}^m_{211}]=0\ . \quad (2.7)$$

The $v(^1S_0,r)$ and $v(^3S_1\text{-}^3D_1,r)$ are the bare NN interactions in these channels, and $\lambda(^1S_0,r)$ and $\lambda(^3S_1\text{-}^3D_1,r)$ are smooth interactions with variational parameters. It is much more convenient to vary the $f^c(r)$, $u^\sigma(r)$, and $u^{t\tau}(r)$ by varying the λ interactions. In the deuteron the optimum correlations are obtained with a constant $\lambda(^3S_1\text{-}^3D_1)=E_d$, the deuteron binding energy; Eq. (2.7) then becomes the deuteron Schrödinger equation. In systems with $A>2$ the spatial dependence of the λ interactions is determined variationally. Physically the λ interactions can be regarded as representing the modifications of the bare NN interaction by other particles in the system.

Variational calculations using the simple Ψ_v given by Eqs. (2.1) and (2.2) have errors of $\approx 10\%$ in the binding energy and radii of ^{3}H and ^{4}He [25,26] compared to exact Faddeev [28] and Green's function Monte Carlo (GFMC) [29] calculations. The most recent variational calculations include two-body correlations with operators $\boldsymbol{\sigma}_i\cdot\boldsymbol{\sigma}_j$, $\boldsymbol{\tau}_i\cdot\boldsymbol{\tau}_j$, $(\boldsymbol{\sigma}_i\cdot\boldsymbol{\sigma}_j)\ (\boldsymbol{\tau}_i\cdot\boldsymbol{\tau}_j)$, S_{ij}, $S_{ij}(\boldsymbol{\tau}_i\cdot\boldsymbol{\tau}_j)$, $\mathbf{L}\cdot\mathbf{S}$, and $\mathbf{L}\cdot\mathbf{S}(\boldsymbol{\tau}_i\cdot\boldsymbol{\tau}_j)$, as well as three-body correlations, and reduce the error in the binding energy to $\approx 3\%$ [23]. The variational wave function also gives electromagnetic form factors in good agreement with the exact Faddeev and GFMC wave functions and the experimental data.

The Δ-isobar components in the nuclear wave function are induced by transition interactions:

$$v_{NN\to N\Delta}=[v^{\sigma\tau\mathrm{II}}(r_{ij})\boldsymbol{\sigma}_i\cdot\mathbf{S}_j+v^{t\tau\mathrm{II}}(r_{ij})S^{\mathrm{II}}_{ij}]\boldsymbol{\tau}_i\cdot\mathbf{T}_j\ , \quad (2.8)$$

$$S^{\mathrm{II}}_{ij}=3(\boldsymbol{\sigma}_i\cdot\hat{\mathbf{r}}_{ij})(\mathbf{S}_j\cdot\hat{\mathbf{r}}_{ij})-\boldsymbol{\sigma}_i\cdot\mathbf{S}_j\ , \quad (2.9)$$

$$v_{NN\to\Delta\Delta}=[v^{\sigma\tau\mathrm{III}}(r_{ij})\mathbf{S}_i\cdot\mathbf{S}_j+v^{t\tau\mathrm{III}}(r_{ij})S^{\mathrm{III}}_{ij}]\mathbf{T}_i\cdot\mathbf{T}_j\ , \quad (2.10)$$

$$S^{\mathrm{III}}_{ij}=3(\mathbf{S}_i\cdot\hat{\mathbf{r}}_{ij})(\mathbf{S}_j\cdot\hat{\mathbf{r}}_{ij})-\mathbf{S}_i\cdot\mathbf{S}_j\ , \quad (2.11)$$

where $\mathbf{S}_i$ and $\mathbf{T}_i$ are transition spin and isospin operators which convert nucleon i into a Δ isobar. Hence the nuclear wave function with Δ-isobar components may be approximated by

$$\Psi=\left[S\prod_{i<j}(1+U^{\mathrm{TR}}_{ij})\right]\Psi_N\ , \quad (2.12)$$

where Ψ_N contains only nucleon degrees of freedom, and the U^{TR}_{ij} are given by

$$U^{\mathrm{TR}}_{ij}=U^{N\Delta}_{ij}+U^{\Delta N}_{ij}+U^{\Delta\Delta}_{ij}\ , \quad (2.13)$$

$$U^{N\Delta}_{ij}=[u^{\sigma\tau\mathrm{II}}(r_{ij})\boldsymbol{\sigma}_i\cdot\mathbf{S}_j+u^{t\tau\mathrm{II}}(r_{ij})S^{\mathrm{II}}_{ij}]\boldsymbol{\tau}_i\cdot\mathbf{T}_j\ , \quad (2.14)$$

$$U^{\Delta\Delta}_{ij}=[u^{\sigma\tau\mathrm{III}}(r_{ij})\mathbf{S}_i\cdot\mathbf{S}_j+u^{t\tau\mathrm{III}}(r_{ij})S^{\mathrm{III}}_{ij}]\mathbf{T}_i\cdot\mathbf{T}_j\ . \quad (2.15)$$

The U^{TR}_{ij} and Ψ_N could be determined variationally by using a Hamiltonian such as the Argonne v_{28} model [22]—that contains both the nucleon and Δ-isobar degrees of freedom—and minimizing the ground-state energy for each given nucleus. Instead we use transition correlations that approximately reproduce two-body bound state and low-energy scattering wave functions for Argonne v_{28}, and assume that these correlations will be relatively A independent, like the nucleonic $u^{t\tau}(r)$ correlations.

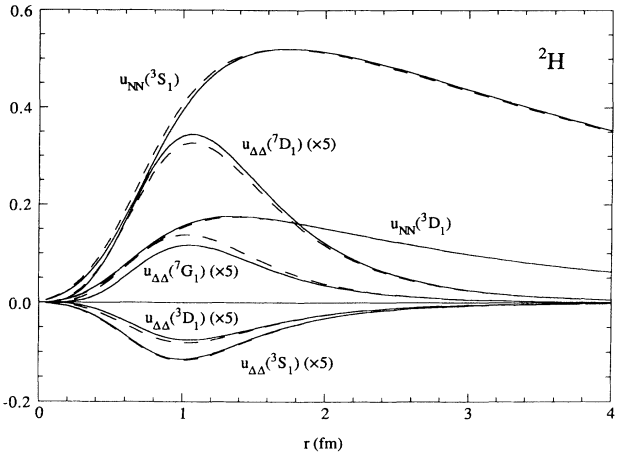

FIG. 2. Comparison of exact and approximate two-body wave functions in the deuteron. Solid lines are exact solutions for the Argonne v_{28} interaction; dashed lines are the approximate fit obtained with Eq. (2.12) using the transition correlations U^{TR}_{ij} and the exact Ψ_N for Argonne v_{14}.

The two-nucleon problem has been exactly solved with the Argonne v_{28} interaction. The two-body wave functions have $N\Delta$ and $\Delta\Delta$ channels at small r_{ij} in addition to the NN channels as shown by the solid lines in Fig. 2 for the deuteron, in Fig. 3 for $^1S_0$ NN scattering at $E_{\mathrm{lab}}=1$ MeV, and in Fig. 4 for $^3P_0$ NN scattering at $E_{\mathrm{lab}}=10$ MeV. These wave functions are very well approximated by the NN channels obtained for the phase-equivalent nucleon-only Argonne v_{14} interaction, and the $N\Delta$ and $\Delta\Delta$ channels obtained from Eq. (2.12), as shown by the

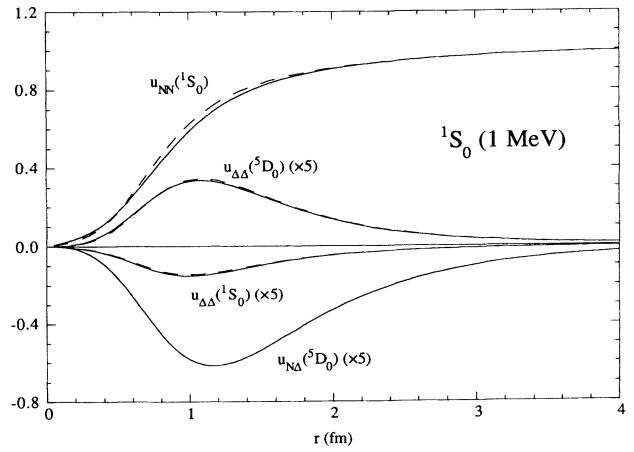

FIG. 3. Comparison of exact and approximate two-body wave functions in $^1S_0$ scattering at $E_{\mathrm{lab}}=1$ MeV. Solid lines are exact solutions for the Argonne v_{28} interaction; dashed lines are the approximate fit obtained with Eq. (2.12) using the transition correlations U^{TR}_{ij} and the exact Ψ_N for Argonne v_{14}.

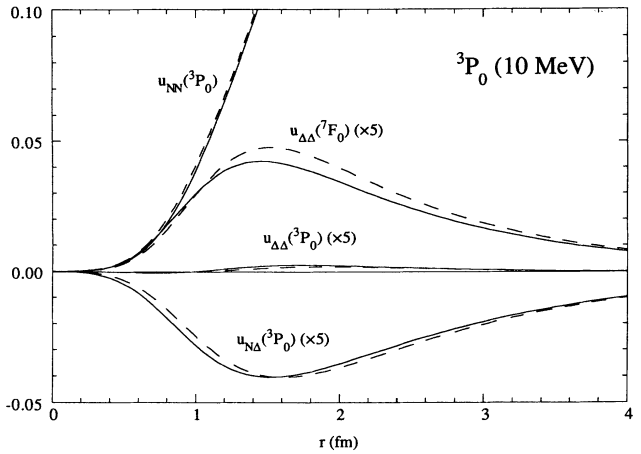

FIG. 4. Comparison of exact and approximate two-body wave functions in $^3P_0$ scattering at $E_{\rm lab}=10$ MeV. Solid lines are exact solutions for the Argonne v_{28} interaction; dashed lines are the approximate fit obtained with Eq. (2.12) using the transition correlations $U_{ij}^{\rm TR}$ and the exact Ψ_N for Argonne v_{14}.

dashed lines in Figs. 2–4. It is important that the Ψ_N used in Eq. (2.12) be proportional to the projected NN channels from the full wave function for the v_{28} interaction, and in Figs. 2–4 it can be seen that they are indeed very similar. In the case of the deuteron, the difference between the v_{14} and v_{28} solutions in the $^3S_1$ NN channel is about the same magnitude as the smallest of the ΔΔ channels, while the difference in the $^3D_1$ NN channels is an order of magnitude smaller.

The transition correlation functions, which are shown in Fig. 5, have been obtained by fitting the $N\Delta$ and ΔΔ wave functions in the deuteron, and in $^1S_0$, $^3P_0$, and $^3P_1$ scattering. The $u^{t\tau\rm II}$ correlation generates the large $^5D_0$ $N\Delta$ component in $^1S_0$ scattering, and is chosen to exactly reproduce the $^5D_0$ wave function. The $u^{\sigma\tau\rm III}$ and $u^{t\tau\rm III}$ correlations generate the $^1S_0$ and $^5D_0$ ΔΔ components in $^1S_0$ scattering and the $^3S_1$, $^3D_1$, $^7D_1$, and $^7G_1$ ΔΔ components of the deuteron. We determine the $u^{\sigma\tau\rm III}$ and $u^{t\tau\rm III}$ by an average fit to these six channels. The $u^{\sigma\tau\rm II}$ correlation only contributes in $S=1,T=1$ channels, and we obtain it from a fit to $N\Delta$ channels in $^3P_0$ and $^3P_1$ NN scattering, with the other transition correlations already fixed.

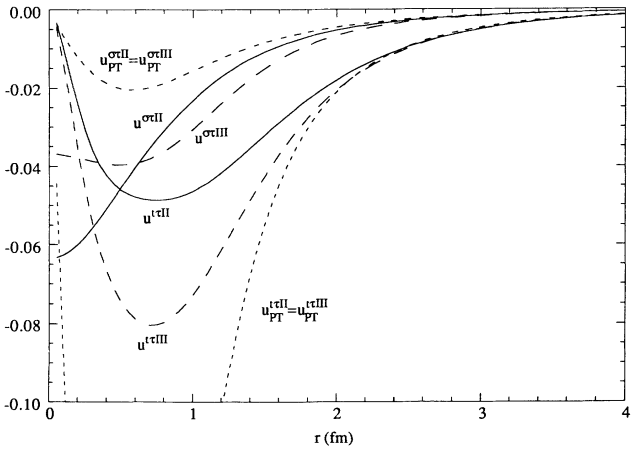

FIG. 5. Transition correlation functions $u^{\sigma\tau\rm II}$, $u^{t\tau\rm II}$ (solid lines), $u^{\sigma\tau\rm III}$, $u^{t\tau\rm III}$ (long dashed lines), and perturbation theory equivalents (short dashed lines); the peak value for $u_{\rm PT}^{t\tau\rm II}$ is −0.27.

One can see in Figs. 2–4 that these transition correlations acting on Ψ_N do a reasonable job of reproducing the actual $N\Delta$ and ΔΔ components. Another measure of the accuracy is the extent to which the bound state or scattering energy is reproduced, as shown in Table I, where the energy components of the deuteron and $^1S_0$ scattering state at $E=0.5$ MeV ($E_{\rm lab}=1$ MeV) is given for both the exact wave function in the v_{28} model, and the approximate wave function of Eq. (2.12). The $N\Delta$ and ΔΔ wave functions are truncated at 12 fm in these calculations, and the integration in the scattering channel is done to the same distance. The total energies and $N\Delta$ interaction energies differ by less than 10%.

The Δ-isobar components in nuclear wave functions are commonly estimated using first-order perturbation theory, and neglecting the kinetic energies in the denominator. Such calculations are equivalent to using Eq. (2.12) for the nuclear wave function with the components of $U_{ij}^{\rm TR}$ given by

$$u_{\rm PT}^{\sigma\tau\rm II}(r_{ij})=\frac{v^{\sigma\tau\rm II}(r_{ij})}{m_N-m_\Delta}\ , \tag{2.16}$$

$$u_{\rm PT}^{t\tau\rm II}(r_{ij})=\frac{v^{t\tau\rm II}(r_{ij})}{m_N-m_\Delta}\ , \tag{2.17}$$

$$u_{\rm PT}^{\sigma\tau\rm III}(r_{ij})=\frac{v^{\sigma\tau\rm III}(r_{ij})}{2(m_N-m_\Delta)}\ , \tag{2.18}$$

$$u_{\rm PT}^{t\tau\rm III}(r_{ij})=\frac{v^{t\tau\rm III}(r_{ij})}{2(m_N-m_\Delta)}\ . \tag{2.19}$$

The correlations $u_{\rm PT}(r)$ are also shown in Fig. 5 for the Argonne v_{28} model, where the coupling constants are such as to give $v^{\sigma\tau\rm III}=2v^{\sigma\tau\rm II}$ and $v^{\sigma\tau\rm III}=2v^{\sigma\tau\rm III}$, hence,

TABLE I. Comparison of energy contributions (in MeV) to the deuteron bound state and $^1S_0$ scattering at $E_{\rm lab}=1$ MeV, as obtained with the exact wave function for the v_{28} model, and the variational wave function using the $U_{ij}^{\rm TR}$ and Ψ_N for the v_{14} model. M, T, and V are the mass difference, kinetic energy, and potential energy contributions to the total energy E. The $V_{\rm rest}=V_{N\Delta\leftrightarrow\Delta N}+V_{N\Delta\leftrightarrow N\Delta}+V_{N\Delta\leftrightarrow\Delta\Delta}+V_{\Delta\Delta\leftrightarrow\Delta\Delta}$.

System	Deuteron		$^1S_0$	
wave function	Exact	Variational	Exact	Variational
$M_{N\Delta}+M_{\Delta\Delta}$	3.08	3.01	1.35	1.35
T_{NN}	19.25	19.10	2.85	3.07
$T_{N\Delta}+T_{\Delta\Delta}$	1.41	1.48	0.90	0.90
$V_{NN\leftrightarrow NN}$	−16.27	−15.66	0.58	0.63
$V_{NN\leftrightarrow N\Delta}$			−4.80	−4.99
$V_{NN\leftrightarrow\Delta\Delta}$	−10.40	−10.62	−1.02	−1.07
$V_{\rm rest}$	0.71	0.69	0.64	0.64
E	−2.22	−2.00	0.50	0.53

$u_{\rm PT}^{\sigma\tau{\rm II}}=u_{\rm PT}^{\sigma\tau{\rm III}}$, and $u_{\rm PT}^{t\tau{\rm II}}=u_{\rm PT}^{t\tau{\rm III}}$. The perturbation theory estimates of the transition tensor correlations are much larger than those calculated in the two-nucleon system, while the transition spin correlations are somewhat smaller.

In this work on three- and four-nucleon systems, the wave functions Ψ_N are calculated for a Hamiltonian containing the Argonne v_{14} two-nucleon [22] and Urbana VIII three-nucleon [23] interaction models. The latter explicitly contains the two-pion-exchange interaction with the Δ-intermediate state, and a phenomenological repulsive term to represent multi-pion-exchange three-nucleon interactions [23–26]. The Δ-isobar components of the wave function are generated with the $U_{ij}^{\rm TR}$ of Fig. 5 calculated for the two-nucleon system. We thus neglect the A dependence of the $U_{ij}^{\rm TR}$ which is presumably a good approximation because the correlations are short ranged, and the nucleonic $u^{t\tau}(r_{ij})$ show very little A dependence. The A dependence of $U_{ij}^{\rm TR}$ is also neglected when first-order perturbation theory is used [2–6,15–17]. The present treatment of Δ-isobar components in the wave function of light nuclei is significantly better than that using first-order perturbation theory, and we expect the error in the present approach to be much less than the difference between it and the perturbation method.

The $NN\rightarrow N\Delta$ and $NN\rightarrow\Delta\Delta$ interactions are not too well known. In the Argonne v_{28} model the long-range transition interaction is assumed to be due to pion exchange. At short range this interaction is cut off with factors that are the same for the $NN\rightarrow NN$, $NN\rightarrow N\Delta$, and $NN\rightarrow\Delta\Delta$ interactions. The published Argonne v_{28} model uses the coupling constants $f_{\pi NN}^2/4\pi=0.081$, $f_{\pi N\Delta}^2/4\pi=0.324$ from Chew-Low theory, and $f_{\pi\Delta\Delta}^2/4\pi=0.00324$ from the static quark model. Note that the Chew-Low value of $\pi N\Delta$ coupling is $\approx 9\%$ smaller than that extracted from the observed Δ-decay width, and that our results are very insensitive to $f_{\pi\Delta\Delta}^2$. We also have an unpublished phase-equivalent potential with the same structure as Argonne v_{28}, but with the quark-model value $f_{\pi N\Delta}^2/4\pi=0.233$, which we designate Argonne v_{28Q} [22]. In the present work we have used the $U_{ij}^{\rm TR}$ calculated from the Argonne v_{28} and v_{28Q} models, with the hope that the difference between the results obtained with these two models may provide an indication of the effect of the uncertainties in the transition interactions.

III. ELECTROMAGNETIC AND AXIAL CURRENT OPERATORS

We expand the electromagnetic or axial current operators into a sum of one- and two-body terms that operate on the nucleon and Δ-isobar degrees of freedom:

$$T_a(\mathbf{q})=\sum_i T_a^{(1)}(i,\mathbf{q})+\sum_{i<j} T_a^{(2)}(ij,\mathbf{q}) , \tag{3.1}$$

where $\mathbf{q}$ is the momentum transferred by the electromagnetic ($a=\gamma$) or weak ($a=\beta$) probe. The one-body term is written as

$$T_a^{(1)}(i,\mathbf{q})=\sum_{B,B'=N,\Delta} T_a(i,\mathbf{q};B\rightarrow B') , \tag{3.2}$$

and is illustrated in Fig. 6. $T_a(N\rightarrow N)$ is the standard single-nucleon electromagnetic or weak current operator, $T_a(N\rightarrow\Delta)$ and $T_a(\Delta\rightarrow N)$ are the current operators associated with the $N\leftrightarrow\Delta$ transitions, and $T_a(\Delta\rightarrow\Delta)$ is the Δ-isobar current. The expressions for $T_a(N\rightarrow N)$ are well known and we have used those given in Refs. [5,6]. The expressions for $T_a(N\rightarrow\Delta)$ are given by

$$T_a(i,\mathbf{q};N\rightarrow\Delta)=\begin{cases} -i\mu_{\gamma N\Delta}\left[\dfrac{e}{2m}\right]\exp(i\mathbf{q}\cdot\mathbf{r}_i)\mathbf{q}\times\mathbf{S}_i T_{z,i}, & a=\gamma , \\ -g_{\beta N\Delta}\exp(i\mathbf{q}\cdot\mathbf{r}_i)\mathbf{S}_i T_{\pm,i}, & a=\beta , \end{cases} \tag{3.3}$$

where $T_\pm=\frac{1}{2}(T_x\pm iT_y)$; the expressions for $T_a(\Delta\rightarrow N)$ are obtained by replacing the transition spin and isospin operators by their Hermitian conjugates.

The transition magnetic moment $\mu_{\gamma N\Delta}$ is taken to be $3\mu_N$, as obtained from the analysis of γN data in the Δ-resonance region [30]. It should be noted that the present value for $\mu_{\gamma N\Delta}$ is about 30% smaller than that predicted by the static quark model [31]. The value of the axial coupling constant $g_{\beta N\Delta}$ is not known, and in this work we have used two choices. In the first the observed tritium β decay is used to determine the value of $g_{\beta N\Delta}$, while in the second $g_{\beta N\Delta}=(6\sqrt{2}/5)g_A$ as predicted by the static quark model [31], with $g_A=1.262$ being the nucleon axial coupling constant [32]. It is worth mentioning that the nucleon can also be excited to a Δ isobar via an electric quadrupole transition, but the associated pion photoproduction amplitude is empirically found to be small at resonance [33]. In any event, the $N\rightarrow\Delta$ quadrupole ($E2$) coupling cannot induce any of the transitions studied here.

The expressions for $T_a(\Delta\rightarrow\Delta)$ are taken as

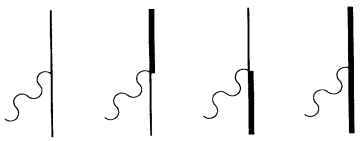

FIG. 6. The current operators $T_a(N\rightarrow N)$, $T_a(N\rightarrow\Delta)$, $T_a(\Delta\rightarrow N)$, and $T_a(\Delta\rightarrow\Delta)$. Thin and thick lines denote nucleons and Δ isobars, respectively.

$$T_a(i,\mathbf{q};\Delta\rightarrow\Delta)=\begin{cases}-i\dfrac{\mu_{\gamma\Delta\Delta}}{12}\left[\dfrac{e}{2m}\right]\exp(i\mathbf{q}\cdot\mathbf{r}_i)\mathbf{q}\times\boldsymbol{\Sigma}_i(1+\theta_{z,i}), & a=\gamma\ ,\\ -g_{\beta\Delta\Delta}\exp(i\mathbf{q}\cdot\mathbf{r}_i)\boldsymbol{\Sigma}_i\theta_{\pm},i, & a=\beta\ ,\end{cases} \tag{3.4}$$

where $\boldsymbol{\Sigma}_i(\theta_i)$ is the Pauli operator for the Δ spin (isospin), $\theta_{\pm}=\frac{1}{2}(\theta_x\pm i\theta_y)$, and the Δ-convection current is neglected. The Δ^{++} magnetic moment $\mu_{\gamma\Delta\Delta}$ is taken to be $4.35\mu_N$, using the average of the values recently obtained from a soft-photon analysis of pion-proton bremsstrahlung data near the Δ^{++} resonance [34]. For the Δ axial coupling constant we use the value $g_{\beta\Delta\Delta}=\frac{9}{5}g_A$, as predicted by the static quark model [31,35]. However, it should be noted that the contributions to the electroweak transition amplitudes associated with $T_a(\Delta\rightarrow\Delta)$ are found to be small for the cases studied here, and hence the final results are not sensitive to the assumed values of $\mu_{\gamma\Delta\Delta}$ and $g_{\beta\Delta\Delta}$.

In the present work we have used only $NN\rightarrow NN$ two-body terms, and their expressions are given and discussed in Refs. [5,6,13,14]. The contributions to $T_\gamma(NN\rightarrow NN)$ are separated into "model-independent" (MI) terms associated with and determined from the NN interaction, and "model-dependent" (MD) terms associated with the $\rho\pi\gamma$ and $\omega\pi\gamma$ electromagnetic couplings. As the axial current operator is not conserved, all the two-body terms $T_\beta(NN\rightarrow NN)$ are to be considered "model dependent." Note that the Δ-isobar current contributions are now explicitly evaluated via $T_a(N\leftrightarrow\Delta)$. In previous work these formed a part of the MD two-body terms. In principle there are also two-body currents associated with the $NN\leftrightarrow N\Delta$ and $NN\leftrightarrow\Delta\Delta$ transitions as illustrated in Fig. 7. However, these have not been included in the present study.

The dominant MI terms are obtained from pseudoscalar and vector components of the interaction. For one-boson-exchange (OBE) potentials these are due to π and ρ exchange. If the Argonne v_{14} and v_{28} models were OBE potentials with identical meson-nucleon coupling constants and form factors, these MI contributions to $T_\gamma(NN\rightarrow NN)$ would be the same in both models. The Argonne v_{14} and v_{28} models are not strictly OBE potentials, however, and their pseudoscalar and vector terms, which are obtained by a projection method, are slightly different. In principle the present calculation should use the MI terms from the v_{28} model, but the results reported here have been obtained with the MI terms from the v_{14} model. We have checked that the trinucleon magnetic moments change very little when MI terms from the v_{28} model are used, as noted in Sec. V.

IV. CALCULATION

In this section we discuss the evaluation of the matrix element of the electroweak transition operator between wave functions that include Δ-isobar components:

$$T_a^{fi}=\frac{\langle\Psi_f|T_a|\Psi_i\rangle}{[\langle\Psi_f|\Psi_f\rangle\langle\Psi_i|\Psi_i\rangle]^{1/2}}\ . \tag{4.1}$$

The initial and final states Ψ_x ($x=i$ or f) have the form of Eq. (2.12). It is convenient to expand these as

$$|\Psi_x\rangle=|\Psi_N^x\rangle+\sum_{i<j}U_{ij}^{\mathrm{TR}}|\Psi_N^x\rangle+\cdots \tag{4.2}$$

and the matrix element of the current operator becomes

$$\langle\Psi_f|T_a|\Psi_i\rangle=\langle\Psi_N^f|T_a(N\text{ only})|\Psi_N^i\rangle+\sum_{\lambda=1,\ldots,5}\langle\Psi_N^f|\sum_{k<l}[T_a(kl)]_\lambda|\Psi_N^i\rangle+(\text{three-body terms})\ , \tag{4.3}$$

where $T_a(N\text{ only})$ denotes all one- and two-body contributions to T_a which only involve nucleon degrees of freedom, namely, $T_a(N\text{ only})=T_a(N\rightarrow N)+T_a(NN\rightarrow NN)$. Its matrix element for the electroweak transitions under consideration has already been calculated in Refs. [5,6,13]. The operators $[T_a]_\lambda$ are illustrated in Figs. 8–10, and are given by

$$[T_a(ij)]_{\lambda=1}=T_a(i;\Delta\rightarrow N)U_{ij}^{\Delta N}+U_{ij}^{\Delta N\dagger}T_a(i;N\rightarrow\Delta)+i\leftrightarrow j\ , \tag{4.4}$$

$$[T_a(ij)]_{\lambda=2}=U_{ij}^{\Delta\Delta\dagger}T_a(i;N\rightarrow\Delta)U_{ij}^{N\Delta}+U_{ij}^{N\Delta\dagger}T_a(i;\Delta\rightarrow N)U_{ij}^{\Delta\Delta}+i\leftrightarrow j\ , \tag{4.5}$$

$$[T_a(ij)]_{\lambda=3}=U_{ij}^{\Delta N\dagger}[T_a(i;\Delta\rightarrow\Delta)+T_a(j;N\rightarrow N)]U_{ij}^{\Delta N}+U_{ij}^{\Delta\Delta\dagger}T_a(i;\Delta\rightarrow\Delta)U_{ij}^{\Delta\Delta}+i\leftrightarrow j\ , \tag{4.6}$$

$$[T_a(ij)]_{\lambda=4}=\left\{U_{ij}^{\Delta N\dagger}\left[\sum_{k\neq i,j}T_a(k;N\rightarrow N)\right]U_{ij}^{\Delta N}+i\leftrightarrow j\right\}+U_{ij}^{\Delta\Delta\dagger}\left[\sum_{k\neq i,j}T_a(k;N\rightarrow N)\right]U_{ij}^{\Delta\Delta}\ , \tag{4.7}$$

$$[T_a(ij)]_{\lambda=5}=\left\{U_{ij}^{\Delta N\dagger}\left[\sum_{k<l\neq i,j}T_a(kl;NN\rightarrow NN)\right]U_{ij}^{\Delta N}+i\leftrightarrow j\right\}+U_{ij}^{\Delta\Delta\dagger}\left[\sum_{k<l\neq i,j}T_a(kl;NN\rightarrow NN)\right]U_{ij}^{\Delta\Delta}\ . \tag{4.8}$$

The terms $[T_a]_{\lambda=1,2,3}$ are two-body current operators. The remaining $[T_a]_{\lambda=4,5}$ are to be interpreted as normalization corrections to the "nucleonic" matrix element $\langle\Psi_N^f|T_a\ (N\text{ only})|\Psi_N^i\rangle$, due to the presence of the Δ-isobar components in the wave function, and occur only in systems in which $A\geq 3$ for $\lambda=4$, or $A\geq 4$ for $\lambda=5$ [36]. Finally, the last term in Eq. (4.3) represents all remaining connected three-body contributions of the type shown in Fig. 11. These are

neglected in the present work, since they are expected to be significantly smaller than those associated with the $[T_a]_\lambda$.

Using the identities for the operators $\mathbf{S}$ and $\mathbf{\Sigma}$,

$$\mathbf{S}^\dagger\cdot\mathbf{A}\,\mathbf{S}\cdot\mathbf{B}=\frac{2}{3}\,\mathbf{A}\cdot\mathbf{B}-\frac{i}{3}\boldsymbol{\sigma}\cdot(\mathbf{A}\times\mathbf{B})\,, \tag{4.9}$$

$$\mathbf{S}^\dagger\cdot\mathbf{A}\,\mathbf{\Sigma}\cdot\mathbf{B}\mathbf{S}\cdot\mathbf{C}=\frac{5}{3}i\,\mathbf{A}\cdot(\mathbf{B}\times\mathbf{C})-\frac{1}{3}\boldsymbol{\sigma}\cdot\mathbf{A}\,\mathbf{B}\cdot\mathbf{C}-\frac{1}{3}\,\mathbf{A}\cdot\mathbf{B}\,\mathbf{C}\cdot\boldsymbol{\sigma}+\frac{4}{3}\,\mathbf{A}\cdot(\mathbf{B}\cdot\boldsymbol{\sigma})\mathbf{C}\,, \tag{4.10}$$

where $\mathbf{A}$, $\mathbf{B}$, and $\mathbf{C}$ are vector operators that commute with $\boldsymbol{\sigma}$, but not necessarily with each other; the $[T_a]_\lambda$ are expressed as operators acting on the nucleon coordinates.

The normalization of the wave function is given by

$$\langle\Psi|\Psi\rangle=\langle\Psi_N|\Psi_N\rangle+\left\langle\Psi_N\left|\sum_{i<j}[2U_{ij}^{\Delta N\dagger}U_{ij}^{\Delta N}+U_{ij}^{\Delta\Delta\dagger}U_{ij}^{\Delta\Delta}]\right|\Psi_N\right\rangle+(\text{three-body terms})\,, \tag{4.11}$$

and the three-body terms have been neglected consistently with the approximation introduced in Eq. (4.3).

The matrix elements in Eqs. (4.3) and (4.11) are computed, without any approximation, by Monte Carlo integration [24]. The wave functions are written as vectors in the spin-isospin space of the A nucleons for any given spatial configuration $\mathbf{R}=\{\mathbf{r}_1,\ldots,\mathbf{r}_A\}$. For the given $\mathbf{R}$, we calculate the state vector $[T_a]_\lambda|\Psi_N\rangle$ by performing exactly the spin-isospin algebra with the techniques described in Ref. [13,24]. The spatial integration is done with the Monte Carlo method by sampling the $\mathbf{R}$ configurations according to the Metropolis algorithm [37].

V. RESULTS

In this section we present our predictions for the magnetic moments of the trinucleons (Tables III and IV), the Gamow-Teller (GT) matrix element of tritium β decay (Tables V and VI), the thermal neutron radiative capture cross section on ^{3}He (Tables VII and VIII), and finally the proton weak capture cross section on ^{3}He at very low (keV) energies (Tables IX and X). In Table II we give the results for the three- and four-body wave function normalizations $\langle\Psi|\Psi\rangle/\langle\Psi_N|\Psi_N\rangle$. The normalization of the $n+{}^3$He or $p+{}^3$He scattering states is the same as that of ^{3}He, up to corrections of order (volume)$^{-1}$. The ground-state and low-energy continuum wave functions of the nucleon component Ψ_N, the model for the one- and two-body parts $T_a(N\rightarrow N)$ and $T_a(NN\rightarrow NN)$ of the electroweak operator, and the variational Monte Carlo (VMC) method used to calculate the required matrix elements have been discussed at length in Refs. [5,6,13,14,23]. Here we shall summarize the essential points.

The variational ground-state wave functions for the three- and four-body systems have been obtained using the Argonne v_{14} two-nucleon plus Urbana VIII three-nucleon interaction model. This Hamiltonian gives the experimental binding energies in exact Faddeev [28] and GFMC [29] calculations; the variational wave functions agree within $\approx 3\%$. The wave functions have fairly large D-state amplitudes: approximately 9% in the trinucleons, and 16% in ^{4}He. The same realistic Hamiltonian and the VMC method are also used to determine the wave functions of the very low-energy continuum $n+{}^3$He and $p+{}^3$He states, with full account of the nucleon-nucleus (including Coulomb) interaction effects [5,6,38]. The $n+{}^3$He and $p+{}^3$He scattering lengths are found to be 3.50 ± 0.25 fm [5] and 10.1 ± 0.5 fm [6], respectively. These are quite close to the values of 3.52 ± 0.25 fm [39] and 10.2 ± 1.4 fm [3,40,41] obtained from effective range parametrizations of $n+{}^3$He and $p+{}^3$He elastic scattering data at low energies. The uncertainties in the calculated values are due to the statistical errors associated with the Monte Carlo integration technique.

In the present work the contributions of the MD two-body currents due to the axial π- and ρ-seagull terms and $\rho\pi$ mechanism (labeled collectively as "mesonic" in

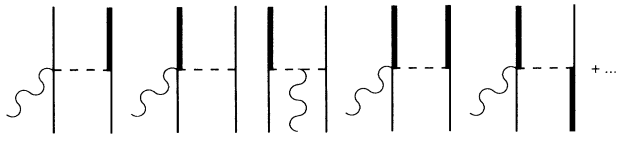

FIG. 7. Some of the two-body exchange-current operators which involve one or more Δ isobars not included in $T_a^{(2)}$. Thin and thick lines denote nucleons and Δ isobars, respectively, while the dashed line represents a π or ρ meson.

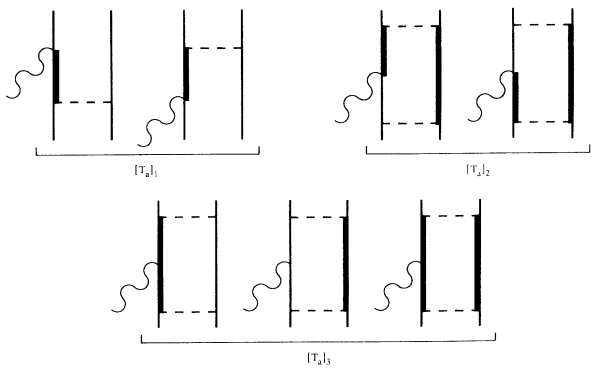

FIG. 8. Diagrams associated with the terms $[T_a]_{\lambda=1,2,3}$. Thin, thick, and dashed lines denote nucleons, Δ-isobars, and transition correlations $U_{ij}^{BB'}$, respectively.

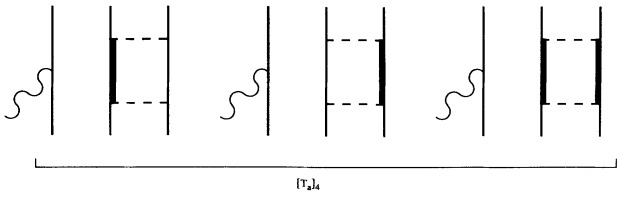

FIG. 9. Diagrams associated with the terms $[T_a]_{\lambda=4}$ in the three-body system. Thin, thick, and dashed lines denote nucleons, Δ-isobars, and transition correlations $U_{ij}^{BB'}$, respectively.

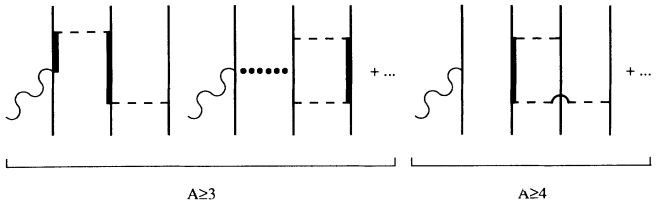

FIG. 11. Diagrams associated with connected three-body terms, which are neglected in the present work. Thin, thick, and dashed lines denote nucleons, Δ-isobars, and transition correlations $U_{ij}^{BB'}$, respectively, while the dotted line represents all two-body exchange contributions included in $T_a(NN\rightarrow NN)$.

Tables V, VI, IX, and X) have been calculated using the cutoff masses $\Lambda_\pi=0.9$ GeV and $\Lambda_\rho=\Lambda_\omega=1.35$ GeV, which were fit to tritium β-decay in Ref. [6]. However, the $\rho\pi\gamma$ and $\omega\pi\gamma$ electromagnetic couplings (in Tables III, IV, VII, and VIII) have been calculated with the previously preferred values $\Lambda_\pi=1.2$ GeV and $\Lambda_\rho=\Lambda_\omega=2.0$ GeV [5]. It should be stressed that there is very little empirical information on the coupling constants (the values used are listed in Refs. [5,6]) and the short-range cutoffs in the mesonic, $\rho\pi\gamma$, and $\omega\pi\gamma$ terms, and therefore their contributions should be viewed as numerically very uncertain.

In Tables III, V, VII, and IX we list the values of the contributions normalized as

$$[\Delta_a]_\lambda=\frac{\langle\Psi_N^f|[T_a]_\lambda|\Psi_N^i\rangle}{[\langle\Psi_N^f|\Psi_N^f\rangle\langle\Psi_N^i|\Psi_N^i\rangle]^{1/2}}\ . \tag{5.1}$$

In Tables IV, VI, VIII, and X the cumulative nucleonic contributions are normalized as

$$\{\mathrm{IA}+\cdots+\omega\pi\gamma\}=\frac{\langle\Psi_N^f|T_a(N\text{ only})|\Psi_N^i\rangle}{[\langle\Psi_N^f|\Psi_N^f\rangle\langle\Psi_N^i|\Psi_N^i\rangle]^{1/2}}\ . \tag{5.2}$$

However, when the isobaric contributions are added to the cumulative sum, the normalization changes to

$$\{\mathrm{IA}+\cdots+\Delta\}=\frac{\langle\Psi_f|T_a(N\text{ only})+\sum_\lambda[T_a]_\lambda|\Psi_i\rangle}{[\langle\Psi_f|\Psi_f\rangle\langle\Psi_i|\Psi_i\rangle]^{1/2}}\ . \tag{5.3}$$

In the tables there are two sets of results for the isobaric contributions which correspond to using the Argonne

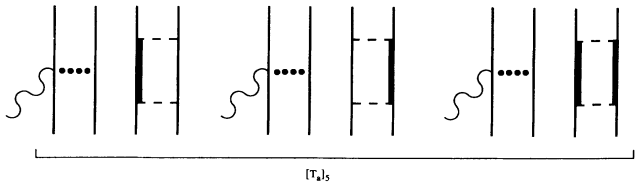

FIG. 10. Diagrams associated with the terms $[T_a]_{\lambda=5}$ in the four-body system. Thin, thick, and dashed lines denote nucleons, Δ-isobars, and transition correlations $U_{ij}^{BB'}$, respectively, while the dotted line represents all two-body exchange contributions included in $T_a(NN\rightarrow NN)$.

v_{28} or v_{28Q} interaction models to generate the transition correlation functions. Furthermore, in the weak transitions the v_{28} values have been calculated with the axial $N\rightarrow\Delta$ coupling constant obtained from tritium β decay, while the v_{28Q} values use the coupling constant from the static model. As already mentioned in Sec. IV, the three-body terms have not been retained in the evaluation of either the matrix elements, Eq. (4.3), or the normalization, Eq. (4.11), as they are expected to produce a small correction. For example, in ^{4}He $\langle\Psi|\Psi\rangle/\langle\Psi_N|\Psi_N\rangle$ is found to be 1.092 without the three-body terms, and 1.103 with them. Finally, the cumulative results quoted in Tables IV, VI, VIII, and X have Monte Carlo statistical errors which are not shown, but are typically less than 1% in the trinucleons, and a few % in the four-body systems.

A. Magnetic moments of the trinucleons

The values quoted for the impulse approximation (IA), "model-independent" (MI), and "model-dependent" (MD) $\rho\pi\gamma$ (isoscalar) and $\omega\pi\gamma$ (isovector) contributions to the trinucleon magnetic moments are the same, within Monte Carlo errors, as those published most recently in Ref. [23]. (Note that in Table VIII of Ref. [23] the values labeled IA+MI+MD include the contribution associated with the $N\rightarrow\Delta$ transition current obtained in perturbation theory by using $u_{\mathrm{PT}}^{\sigma\tau\mathrm{II}}$ and $u_{\mathrm{PT}}^{t\tau\mathrm{II}}$ in $[T_\gamma]_1$.) In that study, the isovector magnetic moment, μ^V, calculated with the variational $|\Psi_N\rangle$, was overestimated by $0.077\mu_N$ (3%). The present study with inclusion of explicit Δ-isobar degrees of freedom in the wave function reduces this overestimate to $0.050\mu_N$ (2%).

As mentioned at the end of Sec. III, it would be more consistent to use MI $NN\rightarrow NN$ contributions derived from the Argonne v_{28} or v_{28Q} interaction. A first calcula-

TABLE II. The ratio $\langle\Psi|\Psi\rangle/\langle\Psi_N|\Psi_N\rangle$, obtained with the Faddeev and variational $|\Psi_N\rangle$.

Interaction model	^{3}He Faddeev	^{3}He variational	^{4}He variational
v_{28}	1.0348	1.0361	1.0919
v_{28Q}	1.0240	1.0249	1.0635

TABLE III. Individual contributions to the isoscalar μ^S and isovector μ^V combinations of the trinucleon magnetic moments associated with the single-nucleon current (IA), the two-body currents that are constructed from the nucleon-nucleon interaction (MI), the $\rho\pi\gamma$ and $\omega\pi\gamma$ mechanisms ($\rho\pi\gamma+\omega\pi\gamma$), and the terms $[T_\gamma]_\lambda$ of Eq. (5.1) ($[\Delta_\gamma]_\lambda$).

	μ^S		μ^V	
	v_{28}	v_{28Q}	v_{28}	v_{28Q}
IA	0.405		−2.187	
MI	0.017		−0.379	
$\rho\pi\gamma+\omega\pi\gamma$	0.006		−0.024	
$[\Delta_\gamma]_1$			−0.056	−0.049
$[\Delta_\gamma]_2$			−0.013	−0.0087
$[\Delta_\gamma]_3$	0.0065	0.0036	−0.011	−0.0063
$[\Delta_\gamma]_4$	0.0091	0.0072	−0.027	−0.019

TABLE IV. Cumulative and normalized contributions to the isoscalar μ^S and isovector μ^V combinations of the trinucleon magnetic moments. The rows labeled IA+ $\cdots$ +$\omega\pi\gamma$ and IA+ $\cdots$ +Δ denote the contributions defined in Eqs. (5.2) and (5.3), respectively.

	μ^S		μ^V	
	v_{28}	v_{28Q}	v_{28}	v_{28Q}
IA	0.405		−2.187	
IA+MI	0.422		−2.566	
IA+ $\cdots$ +$\omega\pi\gamma$	0.428		−2.590	
IA+ $\cdots$ +Δ	0.428	0.428	−2.603	−2.608
Experiment	0.426		−2.553	

TABLE V. Individual contributions to the GT matrix element of tritium β decay associated with the single-nucleon current (IA), the axial π- and ρ-seagull terms, $\rho\pi$ mechanisms (mesonic), and the terms $[T_\beta]_\lambda$ of Eq. (5.1) ($[\Delta_\beta]_\lambda$). They have been divided by g_A. Note that $g_{\beta N\Delta}=2.177g_A$ ($6\sqrt{2}g_A/5$) for v_{28} (v_{28Q}).

	Faddeev		Variational	
	v_{28}	v_{28Q}	v_{28}	v_{28Q}
IA	0.923		0.929	
Mesonic	0.0066		0.0059	
$[\Delta_\beta]_1$	0.0393	0.0270	0.0407	0.0278
$[\Delta_\beta]_2$	0.0093	0.0047	0.0099	0.0049
$[\Delta_\beta]_3$	0.0051	0.0028	0.0054	0.0030
$[\Delta_\beta]_4$	0.0111	0.0076	0.0118	0.0081

TABLE VI. Cumulative and normalized contributions to the GT matrix element of tritium β decay divided by g_A. The row labeled IA+ $\cdots$ +Δ denotes the contributions defined in Eq. (5.3). Note that $g_{\beta N\Delta}=2.177g_A$ ($6\sqrt{2}g_A/5$) for v_{28} (v_{28Q}).

	Faddeev		Variational	
	v_{28}	v_{28Q}	v_{28}	v_{28Q}
IA	0.923		0.929	
IA+mesonic	0.930		0.935	
IA+ $\cdots$ +Δ	0.961	0.949	0.968	0.955
Experiment	0.961			

TABLE VII. Contributions to the matrix element of the radiative capture reaction ^{3}He$(n,\gamma)^4$He at thermal neutron energies. See Table III for notation.

	100 M.E. (fm$^{3/2}$)	
	v_{28}	v_{28Q}
IA	−0.165	
MI	0.756	
$\rho\pi\gamma+\omega\pi\gamma$	0.044	
$[\Delta_\gamma]_1$	0.133	0.117
$[\Delta_\gamma]_2$	0.033	0.021
$[\Delta_\gamma]_3$	0.008	0.004
$[\Delta_\gamma]_4$	−0.123	−0.086
$[\Delta_\gamma]_5$	−0.002	−0.001

TABLE VIII. Cumulative and normalized contributions to the radiative capture reaction ^{3}He$(n,\gamma)^4$He at thermal neutron energies. The two most recent experimental results are also given. See Table IV for notation.

	σ (μb)	
	v_{28}	v_{28Q}
IA	5.65	
IA+MI	72.5	
IA+ · · · +$\omega\pi\gamma$	83.7	
IA+ · · · +Δ	85.9	90.7
Experiment	55±3[a]	
	54±6[b]	

[a]Reference [4].
[b]Reference [7].

TABLE IX. Contributions to the matrix element of the weak capture reaction ^{3}He$(p,e^+\nu_e)^4$He, multiplied by $(\exp(2\pi\eta)-1/2\pi\eta)^{1/2}$, where $\eta=2\alpha/v$, α is the fine-structure constant, and v is the relative p-^{3}He velocity. See Table V for notation.

	M.E. (fm$^{3/2}$)	
	v_{28}	v_{28Q}
IA	0.3849	
Mesonic	0.0137	
$[\Delta_\beta]_1$	−0.2860	−0.1970
$[\Delta_\beta]_2$	−0.0713	−0.0363
$[\Delta_\beta]_3$	−0.0401	−0.0224
$[\Delta_\beta]_4$	0.1855	0.1284
$[\Delta_\beta]_5$	0.0006	0.0004

TABLE X. Cumulative and normalized contributions to the astrophysical S factor of the weak capture reaction ^{3}He$(p,e^+\nu_e)^4$He at zero energy. See Table VI for notation.

	$10^{23}S$ (MeV b)	
	v_{28}	v_{28Q}
IA	6.88	
IA+mesonic	7.38	
IA+ · · · +Δ	1.44	3.14

tion with this change lowers the values in Table IV by 1.7% for μ^S and by 0.4% for μ^V, $0.422\mu_N$ and $-2.589\mu_N$, respectively, for the v_{28} case. Alternatively, if we keep the v_{14} MI terms, but use the more accurate Faddeev $|\Psi_N\rangle$ we get values of $0.426\mu_N$ and $-2.567\mu_N$. In either case, the overestimate of μ^V would be further reduced, to $(0.014–0.036)\mu_N$, or 0.5–1.5 %.

B. Gamow-Teller matrix element of $^3\mathrm{H}\rightarrow{}^3\mathrm{He}+e^-+\bar{\nu}_e$

The results for the IA and mesonic contributions to the Gamow-Teller matrix element of tritium β decay are again consistent within Monte Carlo statistical errors with those published in Ref. [6]. The values reported for the $[\Delta_\beta]_1$ and $[\Delta_\beta]_2$ contributions are obtained by using the coupling constants $g_{\beta N\Delta}=2.177g_A$ and $(6\sqrt{2}/5)g_A$ in the v_{28} and v_{28Q} models, respectively. The former $g_{\beta N\Delta}$ value is obtained by reproducing the empirical GT matrix element of tritium β decay using the Faddeev $|\Psi_N\rangle$, while the latter value is that predicted by the static quark model [31]. It should be noted here that this quark model prediction for $g_{\beta N\Delta}$ was used in Ref. [6] for the $\Delta\pi$ and $\Delta\rho$ contributions listed in Table II of that work. However, the short-range behavior of the axial $N\rightarrow\Delta$ current, i.e., the cutoff masses Λ_π and Λ_ρ in $u_{\mathrm{PT}}^{\sigma\tau\mathrm{II}}$ and $u_{\mathrm{PT}}^{t\tau\mathrm{II}}$, was adjusted by fitting the same empirical matrix element.

C. The ^{3}He$(n,\gamma)^4$He and ^{3}He$(p,e^+\nu_e)^4$He capture reactions

As discussed in Refs. [5,6], the relative smallness of the IA cross section in the ^{3}He$(n,\gamma)^4$He and ^{3}He$(p,e^+\nu_e)^4$He capture reactions is due to the fact that the $T_a(N\rightarrow N)$ operator between the initial $^3S_1$ scattering states and the final ^{4}He state cannot connect the large S-wave components in the ground states of ^{3}He and ^{4}He. Because of this pseudo-orthogonality, only the small components in the wave functions contribute in impulse approximation. Both reactions have large (in the case of radiative neutron capture, dominant) contributions from two-body current operators. The MI and MD mesonic contributions shown here have already been reported in Refs. [5,6]. If MI terms from the v_{28} interaction were used instead, we estimate from the μ^V calculation that the matrix element in Table VII would decrease $\approx 3\%$, and the cross section in Table VIII for the ^{3}He$(n,\gamma)^4$He reaction would decrease $\approx 6\%$.

The contribution $[\Delta_a]_1$ is the leading correction among the Δ-isobar terms. The present value for the radiative (weak) capture matrix element in the v_{28Q} model, 0.117×10^{-2} fm$^{3/2}$ (0.197 fm$^{3/2}$) may be compared to the value of 0.106×10^{-2} fm$^{3/2}$ (-0.22 fm$^{3/2}$) obtained in perturbation theory in Refs. [5,6] by using cutoff masses $\Lambda_\pi=1.2$ GeV and $\Lambda_\rho=2.0$ GeV ($\Lambda_\pi=0.9$ GeV and $\Lambda_\rho=1.35$ GeV) and the static quark model prediction for $f_{\pi N\Delta}$ and $g_{\beta N\Delta}$.

The second leading Δ-isobar contribution is that due to the renormalization correction $[\Delta_a]_4$ of Fig. 9, which as expected has the same sign as the IA matrix element. What may appear surprising is its magnitude; for the v_{28} model, the ratio $[\Delta_a]_4$/IA is ≈ 0.75 (0.48) for radiative

(weak) capture. However, this result is easily understood, when one considers that the operator $[T_a]_4$, in contrast to $T_a(N\rightarrow N)$, has a nonvanishing matrix element between the dominant S-wave components of the ^{3}He and ^{4}He ground states. Finally, the combined contributions $[\Delta_a]_2$ and $[\Delta_a]_3$ amount to $\approx 31\%$ (39%) of the $[\Delta_a]_1$ contribution for radiative (weak) capture. In all earlier calculations the contributions $[\Delta_a]_{2-5}$ were neglected.

Explicit inclusion of Δ-isobar degrees of freedom leads to a significant reduction of the discrepancy between the empirical and theoretical values for the radiative capture cross section than previously reported in Ref. [5], where the calculated cross section was found to be 112 μb. Ignoring the $\omega\pi\gamma$ contribution would reduce the present value of 86 μb for the v_{28} model to 72 μb. No experimental determination of the weak capture cross section is obtainable. The uncertainty in the weak coupling constant $g_{\beta N\Delta}$ introduces a substantial uncertainty in the theoretical prediction for the astrophysical S- factor of this reaction, as reflected in the difference between the v_{28} and v_{28Q} results in Table X. The value of 1.3×10^{-23} MeV b in Ref. [6] is slightly below the range of values quoted in Table X.

VI. DISCUSSION

The present study suggests that the common perturbative treatment of Δ-isobar degrees of freedom in nuclei [2–6,15–17] may not be accurate, and may produce a large overprediction of their importance, particularly in reactions as delicate as the radiative and weak captures on ^{3}He considered here, where the pseudo-orthogonality between the main components of the bound-state wave functions prevents the nucleonic part of the one-body operator from dominating the transition rates. Explicit inclusion of Δ-isobar degrees of freedom in the nuclear wave function influences these transitions in two ways: first, via direct electroweak couplings, and second by renormalization corrections. Whether these effects lead to an enhancement or a quenching of such rates depends on the nature of the particular reaction.

A number of concluding cautionary remarks should be made. First, the $N\Delta$ and $\Delta\Delta$ interactions and the axial $N\rightarrow\Delta$ coupling are not well known. The difference between the calculated v_{28} and v_{28Q} values, particularly for the radiative and weak capture reactions, should provide some estimate of the associated uncertainties—more than a factor of 2 in the latter case.

Second, the capture cross sections show a strong dependence on the scattering length. By varying the $n+^3$He ($p+^3$He) scattering state wave function so that the scattering length ranges from 3.25 fm (9.0 fm) to 3.75 fm (11.0 fm), which is the range given by the data analysis, the radiative (weak) capture cross section varies from ≈ 1.3 (1.2) to ≈ 0.7 (0.8) times the present prediction [5,6]. Obviously, a more accurate experimental determination of the effective range parameters for low-energy $n+^3$He and $p+^3$He elastic scattering data would be useful in ascertaining the quality of the interactions and/or the reliability of the variational description of the continuum states.

Third, there is no compelling evidence for the importance of the poorly known MD $\omega\pi\gamma$ mechanism. If anything, at low momentum transfer its inclusion appears to increase the discrepancy between theory and experiment, as can be seen in Tables IV and VIII. Neglecting this term would give $\mu^V=-2.55\mu_N$ with the Faddeev wave function, and a radiative capture cross section of 72 μb, in significantly better agreement with experiment.

Finally, the cross section of the capture reactions are sensitive to the D-state components of the ^{3}He and ^{4}He ground-state wave functions, and hence to the NN tensor interaction, which is quite strong in the Argonne models. For example, leaving out the D-state wave functions and tensor correlations in the initial scattering state reduces the predicted radiative cross section by $\approx 40\%$. It would be interesting to repeat these calculations with an NN interaction model such as the Nijmegen potential [42], which has a weaker tensor force.

ACKNOWLEDGMENTS

We wish to thank our colleague D. O. Riska for his comments and advice. We also wish to thank C. R. Chen, J. L. Friar, B. F. Gibson, and G. L. Payne for the use of their Faddeev wave function. The calculations reported here were made possible by grants of time on the Cray computers at the National Energy Research Supercomputer Center, Livermore, California, and the National Center for Supercomputing Applications, Urbana, Illinois. The work of J.C. is supported by the U.S. Department of Energy, that of R.S. and R.B.W. by the U.S. Department of Energy, Nuclear Physics Division, under Contract No. W-31-109-ENG-38, and that of V.R.P. by the National Science Foundation, under Grant No. PHY 89-21025.

[1] C. Werntz and J. G. Brennan, Phys. Rev. **157**, 759 (1967); Phys. Rev. C **8**, 1545 (1973).
[2] I. S. Towner and F. C. Khanna, Nucl. Phys. **A356**, 445 (1981).
[3] P. E. Tegnér and C. Bargholtz, Astrophys. J. **272**, 311 (1983).
[4] R. Wervelman, K. Abrahams, H. Postma, J. G. L. Booten, and A. G. M. Van Hees, Nucl. Phys. **A526**, 265 (1991).
[5] J. Carlson, D. O. Riska, R. Schiavilla, and R. B. Wiringa, Phys. Rev. C **42**, 830 (1990).
[6] J. Carlson, D. O. Riska, R. Schiavilla, and R. B. Wiringa, Phys. Rev. C **44**, 619 (1991).
[7] F. L. H. Wolfs, S. J. Freedman, J. E. Nelson, M. S. Dewey, and G. L. Greene, Phys. Rev. Lett. **63**, 2721 (1989).
[8] L. M. Bollinger, J. R. Specht, and G. E. Thomas, Bull. Am. Phys. Soc. **18**, 591 (1973).
[9] M. Suffert and R. Berthollet, Nucl. Phys. **A318**, 54 (1979).
[10] V. P. Alfimenkov, S. B. Borzakov, G. G. Bunatyan, J. Wierzbicki, L. B. Pikel'ner, and É. I. Sharapov, Yad. Fiz. **31**, 21 (1980) [Sov. J. Nucl. Phys. **31**, 10 (1980)].

[11] J. N. Bahcall and R. K. Ulrich, Rev. Mod. Phys. **60**, 297 (1988).
[12] M. Chemtob and M. Rho, Nucl. Phys. **A163**, 1 (1971).
[13] R. Schiavilla, V. R. Pandharipande, and D. O. Riska, Phys. Rev. C **40**, 2294 (1989).
[14] R. Schiavilla and D. O. Riska, Phys. Rev. C **43**, 437 (1991).
[15] J. L. Friar, B. F. Gibson, G. L. Payne, E. L. Tomusiak, and M. Kimura, Phys. Rev. C **37**, 2852 (1988).
[16] J. L. Friar, B. F. Gibson, and G. L. Payne, Phys. Lett. B **251**, 11 (1990).
[17] T.-Y. Saito, Y. Wu, S. Ishikawa, and T. Sasakawa, Phys. Lett. B **242**, 12 (1990).
[18] W. Leidmann and H. Arenhövel, Can. J. Phys. **62**, 1036 (1984); Nucl. Phys. **A465**, 573 (1987).
[19] E. E. van Faassen and J. A. Tjon, Phys. Rev. C **30**, 285 (1984).
[20] R. Dymarz and F. C. Khanna, Phys. Rev. C **41**, 828 (1990).
[21] C. Hadjuk and P. U. Sauer, Nucl. Phys. **A322**, 329 (1979); C. Hadjuk, P. U. Sauer, and W. Streuve, *ibid.* **A405**, 581 (1983).
[22] R. B. Wiringa, R. A. Smith, and T. L. Ainsworth, Phys. Rev. C **29**, 1207 (1984); R. B. Wiringa, unpublished.
[23] R. B. Wiringa, Phys. Rev. C **43**, 1585 (1991).
[24] J. Lomnitz-Adler, V. R. Pandharipande, and R. A. Smith, Nucl. Phys. **A361**, 399 (1981).
[25] J. Carlson, V. R. Pandharipande, and R. B. Wiringa, Nucl. Phys. **A401**, 59 (1983).
[26] R. Schiavilla, V. R. Pandharipande, and R. B. Wiringa, Nucl. Phys. **A449**, 219 (1986).
[27] R. Schiavilla, V. R. Pandharipande, and D. O. Riska, Phys. Rev. C **41**, 309 (1990).
[28] C. R. Chen, G. L. Payne, J. L. Friar, and B. F. Gibson, Phys. Rev. C **33**, 1740 (1986); and private communication (1990).
[29] J. Carlson, Phys. Rev. C **38**, 1879 (1988); Los Alamos Report No. LA-UR-90-2088 (1990).
[30] C. E. Carlson, Phys. Rev. D **34**, 2704 (1986).
[31] G. E. Brown and W. Weise, Phys. Rep. **22**, 279 (1975).
[32] P. Bopp, D. Dubbers, L. Hornig, E. Klemt, J. Last, H. Schütze, S. J. Freedman, and O. Schärpf, Phys. Rev. Lett. **56**, 919 (1986).
[33] T. E. O. Ericson and W. Weise, *Pions and Nuclei* (Clarendon Press, Oxford, 1988).
[34] D. Lin and M. K. Liou, Phys. Rev. C **43**, R930 (1991).
[35] D. O. Riska, private communication.
[36] A. M. Green and T. Schucan, Nucl. Phys. **A188**, 289 (1972).
[37] N. Metropolis, A. W. Rosenbluth, M. N. Rosenbluth, A. H. Teller, and E. Teller, J. Chem. Phys. **21**, 1087 (1953).
[38] J. Carlson, K. E. Schmidt, and M. H. Kalos, Phys. Rev. C **36**, 27 (1987).
[39] H. Kaiser, H. Rauch, W. Bauspiess, and U. Bonse, Phys. Lett. **71B**, 321 (1977).
[40] T. A. Tombrello, Phys. Rev. **138**, B40 (1965).
[41] H. Berg, W. Arnold, E. Huttel, H. H. Krause, J. Ulbricht, and G. Clausnitzer, Nucl. Phys. **A334**, 21 (1980).
[42] M. M. Nagels, T. A. Rijken, and J. J. de Swart, Phys. Rev. D **17**, 768 (1978).